Available online at www.sciencedirect.com
SCIENCE DIRECT®
Solid State Sciences 8 (2006) 836–842
Solid State Sciences
www.elsevier.com/locate/ssscie

Crystal structure and magnetic properties of $Co_7(TeO_3)_4Br_6$—a new cobalt tellurite bromide

Richard Becker [a,*], Mats Johnsson [a], Helmuth Berger [b], Mladen Prester [c], Ivica Zivkovic [c], Djuro Drobac [c], Marko Miljak [c], Mirta Herak [c]

[a] *Department of Inorganic Chemistry, Stockholm University, S-106 91 Stockholm, Sweden*
[b] *Institut de Physique de la Matiere Complexe, Ecole Polytechnique Fédérale de Lausanne, CH-1015 Lausanne, Switzerland*
[c] *Institute of Physics, POB 304, HR-10000 Zagreb, Croatia*

Received 20 January 2006; accepted 24 March 2006

Available online 5 June 2006

Abstract

The crystal structure of the new compound $Co_7(TeO_3)_4Br_6$ is described together with the magnetic properties. The new compound crystallizes in the monoclinic space group C2/c with the unit cell parameters $a = 20.6532(5)$ Å, $b = 8.6533(2)$ Å, $c = 14.7262(5)$ Å, $\beta = 124.897(3)°$, $Z = 4$. The crystal structure was solved from single crystal data, $R = 0.0242$. The structure can be considered as layered and the building units are $[CoO_4Br_2]$ and $[CoO_2Br_4]$ octahedra and $[TeO_3E]$ tetrahedra, E being the $5s^2$ lone pair on the Te(IV) ions. The magnetic properties of the compound are characterised by antiferromagnetic correlations at high temperatures, strong deviation from the Curie–Weiss behaviour in a broad intermediate temperature range and long range magnetic ordering setting-in at low temperatures. Magnetic ordering takes place in stages, being represented by two susceptibility anomalies, at $T_N = 33$ K and $T_C = 27$ K. The magnetic transition at T_C is ferromagnetic (or ferrimagnetic) in character.
© 2006 Elsevier SAS. All rights reserved.

Keywords: Cobalt; Oxohalide; Stereochemically active lone pair; Magnetic ordering; Antiferromagnetic; Ferromagnetic

1. Introduction

Cations of p-elements that have a stereochemically active lone electron pair, e.g., Te^{4+}, Se^{4+}, As^{3+} and Sb^{3+}, often adopt an asymmetric or one-sided coordination to oxygen ions. If the lone pair, designated E, is taken into account the coordination can most often be described as tetrahedral, e.g., $[SeO_3E]$, or trigonal bipyramidal, e.g., $[TeO_4E]$.

The family of transition metal tellurite halides has proved to show great promise for finding low-dimensional compounds or quantum spin systems [1–5]. In particular, the transition metal tellurite halides relying on Cu^{2+}, $S = 1/2$, ions manifests magnetism of intriguing complexity, revealing a number of exciting new magnetic phenomena [6,7]. The low spin number of Cu^{2+}, enhancing the role of quantum fluctuations, is partially responsible for these findings.

Late transition metal cations coordinate to both oxygen and halide anions while lone-pair cations most often form bonds only to oxygen anions in the family of oxohalides; this difference in chemical affinity will further assist in the formation of low-dimensional compounds. However, oxofluorides has been excluded from the studies as the high electronegativity of F^- means that it regularly forms bonds to both late transition metal cations and to lone-pair cations.

From the viewpoint of fundamental magnetism there is a natural interest for synthesis and studies of non-copper-based transition metal tellurite halides. Due to the diversity of its spin states, cobalt seems as a good candidate. Although pronounced quantum fluctuations are not expected in systems revealing spin numbers larger than $S = 1$, interesting magnetism may generally arise from reduced magnetic dimensionality or connectivity, or from geometrically imposed frustration and/or specific topology [8].

Two cobalt(II) tellurite-halide compounds are hitherto known; $Co_2TeO_3X_2$ ($X = Cl, Br$) and $Co_6(TeO_3)_2(TeO_6)Cl_2$,

* Corresponding author. Tel.: +46 8 16 24 34.
E-mail address: richard@inorg.su.se (R. Becker).

1293-2558/$ – see front matter © 2006 Elsevier SAS. All rights reserved.
doi:10.1016/j.solidstatesciences.2006.03.004

the latter having mixed oxidation states on tellurium [9,10]. The objective of the present work was to further investigate the system Co^{2+}–Te^{4+}–O–X and it resulted in the discovery of the isostructural compounds $Co_7(TeO_3)_4Br_6$ and $Co_7(TeO_3)_4Cl_{3.6}Br_{2.4}$. The crystal structures and magnetic properties are discussed.

2. Experimental

2.1. Synthesis and crystal growth

The new compounds $Co_7(TeO_3)_4Br_6$ and $Co_7(TeO_3)_4Cl_{3.6}Br_{2.4}$ were synthesized via chemical vapor transport reactions. The starting materials were CoO (Alfa Aesar 99.999%), TeO_2 (Acros 99%) and $CoBr_2$ (Alfa Aesar 99.9%). The single crystals used in this study were grown from mixtures of CoO, TeO_2, and $CoBr_2$ in the off-stoichiometric molar ratio 4 : 3 : 2.

The starting powders were mixed in an agate mortar, and placed in silica ampoules that were sealed after evacuation to 10^{-5} Torr. The ampoules were heated slowly to 500 °C in a horizontal electric furnace and held there for four days followed by slow cooling by 50 °C/h to room temperature. This heating procedure was repeated three times. The resulting sintered powder was blue and poly-phasic, and its phase composition was not analyzed. Single crystals of the new compounds were prepared by chemical vapor transport from the sintered powder as detailed below.

For the $Co_7(TeO_3)_4Br_6$ single crystals, a portion (about 10–20 g) of powder of the primary reaction product was enclosed in evacuated (10^{-5} Torr) and sealed silica ampoules, along with electronic grade HBr as transporting agent. The size of the ampoule does not appear to be a determining factor. Typical dimensions were 20–35 mm for the diameter and 200–250 mm for the length. The choice of the length is related with the profile of the temperature gradient. Small gradients between the source and the growth zones produce a slower transport and usually smaller size and less number of crystals, however of higher quality.

The ampoules were then placed in two zone gradient furnaces. Charge and growth-zone temperatures were 600 and 400 °C respectively. After some few weeks purple platelets with a size of $10 \times 10 \times 0.1$ mm^{-3} of $Co_7(TeO_3)_4Br_6$ had grown in the center of the ampoule. The ampoule also contained an uncharacterized blue powder.

For the $Co_7(TeO_3)_4Cl_{3.6}Br_{2.4}$ single crystals, about 20 g of the prepared powder mixture described above was placed in a silica tube and subsequently evacuated. Electronic grade HCl was added in sufficient quantity and used as transporting agent. The ampoule was placed in a two zone gradient furnace, where charge and growth-zone temperatures were 600 and 450 °C respectively. After four weeks, the formation of purple platelet crystals with a size of $15 \times 10 \times 0.1$ mm^{-3} of $Co_7(TeO_3)_4Cl_{3.6}Br_{2.4}$ had grown in the center of the ampoule together with an uncharacterized blue powder.

The synthesis products were characterized in a scanning electron microscope (SEM, JEOL 820) with an energy-dispersive spectrometer (EDS, LINK AN10000) confirming the presence and stoichiometry of Co, Te, Br and Cl.

2.2. Crystal structure determination

Single-crystal X-ray data were collected on an Oxford Diffraction Xcalibur3 diffractometer using graphite-monochromatized Mo K_α radiation, $\lambda = 0.71073$ Å. The intensities of the reflections were integrated using the software supplied by the manufacturer. Numerical absorption correction was performed with the programs X-red [11] and X-shape [12]. The crystal structures were solved by direct methods using the program SHELXS97 [13] and refined by full matrix least squares on F^2 using the program SHELXL97 [14]. All atoms are refined with anisotropic displacement parameters. Experimental parameters for $Co_7(TeO_3)_4Br_6$ are reported in Table 1.

2.3. Magnetic susceptibility measurements

Magnetic AC susceptibility data were measured with a CryoBIND system. The measuring amplitude of the applied AC magnetic fields was relatively small (at the order of 1 Oe). Magnetic dc susceptibility was measured by the Faraday balance method in the measuring field of 5 kG.

Table 1
Crystal data for $Co_7(TeO_3)_4Br_6$

Empirical formula	$Co_7(TeO_3)_4Br_6$
Formula weight	1594.37
Temperature	292(3) K
Wavelength	0.71073
Crystal system	Monoclinic
Space group	C2/c
Unit cell dimensions	$a = 20.6532(5)$ Å
	$b = 8.6533(2)$ Å
	$c = 14.7262(5)$ Å
	$\beta = 124.897(3)°$
Volume (Å^3)	2136.1(1)
Z	4
Density (calculated)	4.598 g cm^{-3}
Absorption coefficient	21.927 mm^{-1}
Absorption correction	Numerical
$F(000)$	2812
Crystal colour	Purple
Crystal habit	Thin flakes
Crystal size (mm)	$0.182 \times 0.075 \times 0.020$ mm^3
θ range for data collection	3.81–30.92°
Index ranges	$-29 \leqslant h \leqslant 29$
	$-12 \leqslant k \leqslant 12$
	$-21 \leqslant l \leqslant 21$
Reflections collected	18179
Independent reflections	3403 [$R_{int} = 0.0368$]
Completeness to $\theta = \max$ °	99%
Refinement method	Full-matrix least squares on F^2
Data/restraints/parameters	3403/0/134
Goodness-of-fit on F^2	1.158
Final R indices [$I > 2\theta(I)$]	$R1 = 0.0242$
	$wR2 = 0.0549$
R indices (all data)	$R1 = 0.0309$
	$wR2 = 0.0575$
Largest diff. peak and hole	2.712 and −1.715 (e Å^{-3})

Single crystalline platelets were used in the AC susceptibility studies, the platelets were $2 \times 2 \times 0.1$ mm and had irregular shapes. Powdered single crystals were used in the dc susceptibility studies.

3. Results

3.1. Crystal structure

The compound $Co_7(TeO_3)_4Br_6$ crystallise in the monoclinic space group C2/c. Experimental parameters, atomic coordinates and selected interatomic distances and angles are reported in Tables 1, 2 and 3 respectively. The presence and stoichiometry of the heavier elements has been confirmed by EDS analysis

Table 2
Atomic coordinates and equivalent isotropic displacement parameters for $Co_7(TeO_3)_4Br_6$

Atom	Wyck.	x	y	z	U_{eq} [a] [Å^2]
Te(1)	*8f*	0.38278(2)	0.49309(2)	0.09860(2)	0.1092(6)
Te(2)	*8f*	0.17521(2)	0.50214(2)	0.13890(2)	0.1073(6)
Co(1)	*8f*	0.33382(3)	0.39817(5)	0.33796(3)	0.0136(1)
Co(2)	*8f*	0.29264(3)	0.80871(5)	0.12419(3)	0.01205(9)
Co(3)	*8f*	0.29151(3)	0.18493(5)	0.12119(4)	0.0148(1)
Co(4)	*4a*	1/2	1/2	1/2	0.0244(2)
Br(1)	*8f*	0.41008(3)	0.68781(4)	0.32411(3)	0.0272(1)
Br(2)	*8f*	0.44858(2)	0.25849(4)	0.34912(3)	0.02023(8)
Br(3)	*8f*	0.38722(2)	−0.01450(4)	0.11478(3)	0.01742(8)
O(1)	*8f*	0.2229(2)	0.5044(2)	0.2983(2)	0.0119(4)
O(2)	*8f*	0.2116(2)	0.7026(2)	0.1427(2)	0.0137(4)
O(3)	*8f*	0.2648(2)	0.3897(2)	0.1717(2)	0.0137(4)
O(4)	*8f*	0.3018(2)	0.6367(2)	0.0408(2)	0.0137(4)
O(5)	*8f*	0.3169(2)	0.3210(2)	0.0299(2)	0.0152(5)
O(6)	*8f*	0.4044(2)	0.5304(3)	−0.0082(2)	0.0140(4)

[a] U_{eq} is defined as one-third of the trace of the orthogonalized U tensor.

Table 3a
Selected bond lengths (Å) for $Co_7(TeO_3)_4Br_6$

Te(1)–O(4)	1.845(2)	Co(2)–O(2)	2.056(2)
Te(1)–O(5)	1.863(2)	Co(2)–O(4)	1.995(2)
Te(1)–O(6)	1.891(2)	Co(2)–O(4)^{iii}	2.122(2)
Te(2)–O(1)	1.958(2)	Co(2)–Co(2)^{iii}	3.181(5)
Te(2)–O(2)	1.862(2)	Co(2)–Co(3)^{v}	3.222(1)
Te(2)–O(3)	1.888(2)	Co(3)–Br(2)	3.1189(6)
Co(1)–Br(1)	3.0069(6)	Co(3)–Br(3)	2.6545(6)
Co(1)–Br(2)	2.5748(6)	Co(3)–O(1)^{ii}	2.071(2)
Co(1)–O(1)	2.211(2)	Co(3)–O(3)	2.098(2)
Co(1)–O(2)^{ii}	2.017(2)	Co(3)–O(5)	2.061(2)
Co(1)–O(3)	2.009(2)	Co(3)–O(5)^{vi}	2.066(2)
Co(1)–O(6)^{i}	1.963(2)	Co(3)–Co(3)^{vi}	3.150(5)
Co(1)–Co(2)^{ii}	3.063(1)	Co(4)–Br(1)	2.6909(4)
Co(1)–Co(3)	3.331(2)	Co(4)–Br(1)^{viii}	2.6909(4)
Co(1)–Co(4)	2.977(1)	Co(4)–Br(2)	2.7644(3)
Co(2)–Br(1)	2.7298(6)	Co(4)–Br(2)^{viii}	2.7644(3)
Co(2)–Br(3)^{v}	2.5370(5)	Co(4)–O(6)^{i}	1.927(2)
Co(2)–O(1)^{iv}	2.153(2)	Co(4)–O(6)^{vii}	1.927(2)

Symmetry transformations used to generate equivalent atoms:
^{i} $x, 1-y, 0.5+z$; ^{ii} $0.5-x, -0.5+y, 0.5-z$; ^{iii} $0.5-x, 1.5-y, -z$; ^{iv} $0.5-x, 0.5+y, 0.5-z$; ^{v} $x, 1+y, z$; ^{vi} $0.5-x, 0.5-y, -z$; ^{vii} $1-x, y, 0.5-z$ ^{viii} $1-x, 1-y, 1-z$.

Table 3b
Selected bond angles (°) for $Co_7(TeO_3)_4Br_6$

O(4)–Te(1)–O(5)	95.1(1)	O(4)^{iii}–Co(2)–Br(1)	170.35(6)
O(4)–Te(1)–O(6)	95.0(1)	O(4)^{iii}–Co(2)–Br(3)^{v}	92.20(6)
O(5)–Te(1)–O(6)	97.4(1)	O(4)^{iii}–Co(2)–O(1)^{iv}	96.75(8)
O(2)–Te(2)–O(3)	98.2(1)	Br(3)–Co(3)–Br(2)	80.27(2)
O(2)–Te(2)–O(1)	92.12(9)	O(1)^{ii}–Co(3)–Br(2)	86.32(7)
O(3)–Te(2)–O(1)	87.21(9)	O(1)^{ii}–Co(3)–Br(3)	83.90(6)
Br(2)–Co(1)–Br(1)	83.62(2)	O(1)^{ii}–Co(3)–O(3)	105.54(8)
O(1)–Co(1)–Br(1)	98.42(5)	O(3)–Co(3)–Br(2)	76.28(7)
O(1)–Co(1)–Br(2)	170.08(6)	O(3)–Co(3)–Br(3)	154.47(7)
O(2)^{ii}–Co(1)–Br(1)	176.42(7)	O(5)–Co(3)–Br(2)	95.26(7)
O(2)^{ii}–Co(1)–Br(2)	95.19(7)	O(5)–Co(3)–Br(3)	82.42(6)
O(2)^{ii}–Co(1)–O(1)	83.33(9)	O(5)–Co(3)–O(1)^{ii}	165.76(9)
O(3)–Co(1)–Br(1)	88.91(6)	O(5)–Co(3)–O(3)	88.58(8)
O(3)–Co(1)–Br(2)	92.65(7)	O(5)–Co(3)–O(5)^{vi}	80.5(1)
O(3)–Co(1)–O(1)	77.73(9)	O(5)^{vi}–Co(3)–Br(2)	169.53(6)
O(3)–Co(1)–O(2)^{ii}	94.52(9)	O(5)^{vi}–Co(3)–Br(3)	108.43(6)
O(6)^{i}–Co(1)–Br(1)	75.50(7)	O(5)^{vi}–Co(3)–O(1)^{ii}	100.17(9)
O(6)^{i}–Co(1)–Br(2)	91.31(7)	O(5)^{vi}–Co(3)–O(3)	93.44(9)
O(6)^{i}–Co(1)–O(1)	98.60(9)	Br(1)–Co(4)–Br(2)	86.40(1)
O(6)^{i}–Co(1)–O(2)^{ii}	101.18(9)	Br(1)–Co(4)–Br(2)^{viii}	93.60(1)
O(6)^{i}–Co(1)–O(3)	163.39(9)	Br(1)^{viii}–Co(4)–Br(1)	180.0
Br(3)^{v}–Co(2)–Br(1)	92.77(2)	Br(1)^{viii}–Co(4)–Br(2)	93.60(1)
O(1)^{iv}–Co(2)–Br(1)	91.90(6)	Br(1)^{viii}–Co(4)–Br(2)^{viii}	86.40(1)
O(1)^{iv}–Co(2)–Br(3)^{v}	85.25(6)	Br(2)–Co(4)–Br(2)^{viii}	180.0
O(2)–Co(2)–Br(1)	88.72(7)	O(6)^{i}–Co(4)–Br(1)	84.40(7)
O(2)–Co(2)–Br(3)^{v}	169.11(6)	O(6)^{i}–Co(4)–Br(1)^{viii}	95.60(7)
O(2)–Co(2)–O(1)^{iv}	83.92(9)	O(6)^{i}–Co(4)–Br(2)	86.57(6)
O(2)–Co(2)–O(4)^{iii}	87.96(9)	O(6)^{i}–Co(4)–Br(2)^{viii}	93.43(6)
O(4)–Co(2)–Br(1)	92.60(7)	O(6)^{i}–Co(4)–O(6)^{vii}	180.0
O(4)–Co(2)–Br(3)^{v}	93.42(7)	O(6)^{vii}–Co(4)–Br(1)	95.60(7)
O(4)–Co(2)–O(1)^{iv}	175.37(9)	O(6)^{vii}–Co(4)–Br(1)^{viii}	84.40(7)
O(4)–Co(2)–O(2)	97.29(3)	O(6)^{vii}–Co(4)–Br(2)	93.43(6)
O(4)–Co(2)–O(4)^{iii}	78.85(9)	O(6)^{vii}–Co(4)–Br(2)^{viii}	86.57(6)

Symmetry transformations used to generate equivalent atoms:
^{i} $x, 1-y, 0.5+z$; ^{ii} $0.5-x, -0.5+y, 0.5-z$; ^{iii} $0.5-x, 1.5-y, -z$; ^{iv} $0.5-x, 0.5+y, 0.5-z$; ^{v} $x, 1+y, z$; ^{vi} $0.5-x, 0.5-y, -z$; ^{vii} $1-x, y, 0.5-z$ ^{viii} $1-x, 1-y, 1-z$.

which gives; 38.9 at% Co, 23.2 at% Te and 37.9 at% Br which is in good agreement with the structure refinement that gives; 41.2 at% Co, 23.5 at% Te and 35.3 at% Br.

Attempts to synthesize a Cl-analogue failed, but the mixed halide compound $Co_7(TeO_3)_4Cl_{3.6}Br_{2.4}$ was found. It is isostructural with the Br-analogue and the unit cell was found to be $a = 20.6724$, $b = 8.4932$, $c = 14.6326$ Å, and $\beta = 125.77°$. EDS analysis on ten crystals gave as average; 37.7 at% Co, 23.6 at% Te, 22.4 at% Cl, and 16.2 at% Br. This indicate that the halide positions are occupied by 58% Cl and 42% Br. Structural refinement of the Cl/Br occupancy using single crystal X-ray diffraction data yielded the composition $Co_7(TeO_3)_4Cl_{3.6}Br_{2.4}$ which means 60% Cl and 40% Br at the halide positions which thus is in very good agreement with EDS data. As the two compounds are isostructural the crystal structure of the mixed Cl/Br compound will not be further discussed in this article.

The two crystallographically different Te^{4+} cations both have tetrahedral $[TeO_3E]$ coordination with Te–O distances in the range 1.845–1.958 Å. In many tellurites and tellurite-halides there is also a forth oxygen present with a Te–O distance in be-

tween 2 and 3 Å [1,15,16], however, such a forth oxygen is not present in the new compound making it likely that there also exist a Se^{4+} analogue as the $[SeO_3E]$ coordination is dominating in selenites and selenite-halides [17–19].

There are four crystallographically different Co positions in the structure. Three of these have octahedral coordination where the two Br ions are cis-positioned to each other. The fourth Co^{2+} cation has an octahedral $[Co(4)O_2Br_4]$ coordination with all four Br anions positioned in the square plane, see Fig. 1.

The structure can be described as layered in the *bc*-plane. The cobalt polyhedra in the layers are connected so that two types of weaving chains (A and A′) extend along the *b*-direction. The chains are built by groups of two edge sharing $[Co(2)O_4Br_2]$ and groups of two egde sharing $[Co(3)O_4Br_2]$ polyhedra. These chains are then connected via corner and edge sharing to $[Co(1)O_4Br_2]$ octahedra and via corner sharing to $[TeO_3E]$ tetrahedra to form the layers, see Fig. 2. The layers are then joined by $[Co(4)O_2Br_4]$ octahedra, see Fig. 3. The lone-pairs protrude out from the layers into non-bonding regions were also the Br atoms are located, see Fig. 3. Such non-bonding regions are common in tellurite halide compounds [1,9,10].

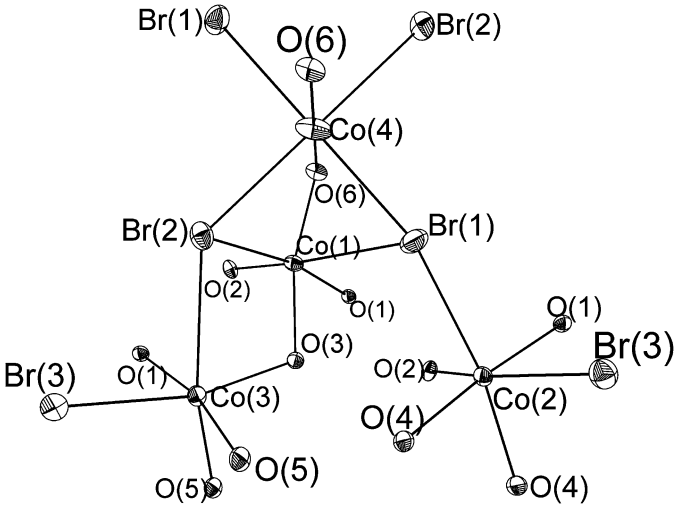

Fig. 1. The coordination around the four crystallographically different Co^{2+} cations with ellipsoids drawn at the 50% probability level.

3.2. Magnetic properties

Magnetic susceptibilities of the $Co_7(TeO_3)_4Br_6$ system have been studied by both DC- and AC-susceptibility techniques. Temperature dependence of DC-susceptibility, represented by its inverse $1/\chi$, is shown in Fig. 4. Obviously, there are three characteristic ranges—a Curie–Weiss (CW) type of temperature dependence, $1/\chi = (T - \theta_{CW})/C$, obeyed at high temperatures (above 150 K), a systematic downturn deviation from the CW behaviour in the intermediate temperature range (35 K < T < 150 K) while below 35 K there are clear indications of magnetic orderings. In the high temperature CW-regime linear data fit provides the value of the Curie constant, C = 20.4 emu·K/mol. The effective number of Bohr magnetons μ_{eff} $(= (3k_BC/(N_M\mu_B^2))^{1/2})$ is therefore $\mu_{eff} \approx 4.8$ coinciding with the characteristic experimental value for Co^{2+} ions in diluted magnetic systems [20]. Considering the $3d^7$ orbital configuration of Co^{2+} the latter result is compatible with the high-spin $S = 3/2$ ground state favoured by Hund's rules [20]. However, the related g-factor ($g \approx 2.5$) deviates from the free electron

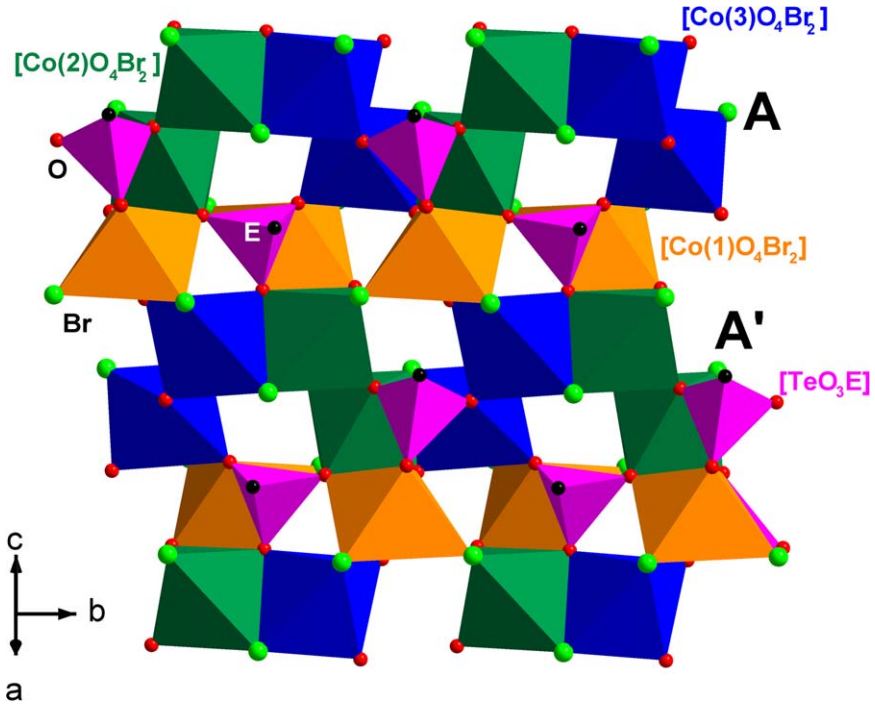

Fig. 2. One layer of $Co_7(TeO_3)_4Br_6$ built up by two different chains of $[CoO_4Br_2]$ octahedra marked A and A′. The chains are connected to form layers via the $[Co(1)O_4Br_2]$ octahedra and the $[TeO_3E]$ tetrahedra. View along the [101] direction.

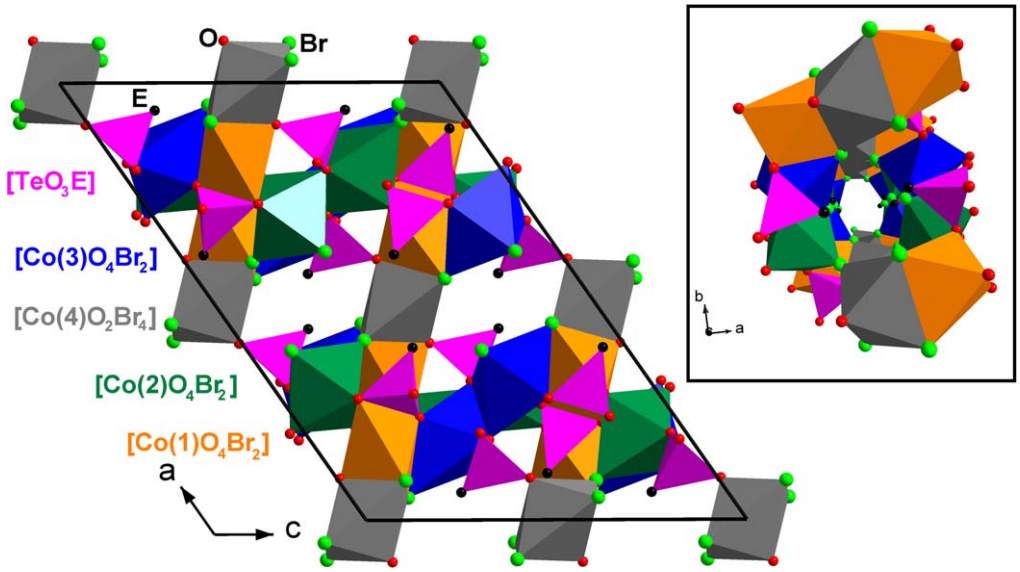

Fig. 3. The structure of $Co_7(TeO_3)_4Br_6$ were the layers are made up of $[TeO_3E]$ tetrahedra and different Co(1), Co(2) and Co(3) octahedra, which are connected via the Co(4) octahedra. The inset shows channels on non-bonding regions running along the [001] direction.

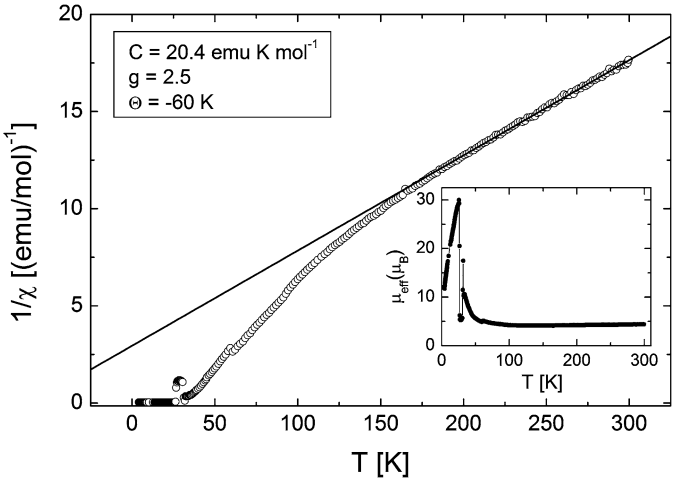

Fig. 4. Curie–Weiss fit of measured DC susceptibility of powdered $Co_7(TeO_3)_4Br_6$ single crystals. Parameters consistent with the high-temperature Curie–Weiss behaviour are shown in the top panel. Bottom inset illustrates the temperature dependence of the effective number of Bohr magnetons (see, main text).

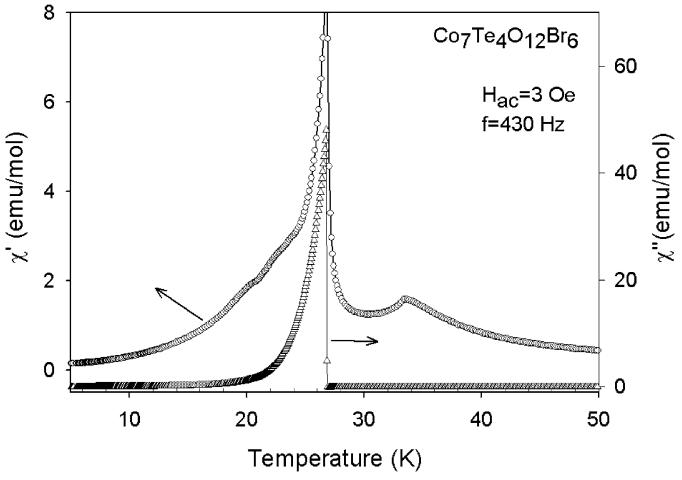

Fig. 5. AC susceptibility of single-crystalline sample (sample mass 1.6 mg) in the magnetic ordering transition temperature region. Results for both real (χ', circles) and imaginary (χ'', triangles) susceptibility are shown. The solid line connects the χ''-data points. The ferromagnetic (or ferrimagnetic) transition at 27 K is accompanied by unusually big and extremely sharp imaginary susceptibility peak.

value ($g \approx 2$) revealing incomplete quenching of the orbital degrees of freedom and the importance of crystal (ligand) field effects. Pronounced deviation from CW behaviour in the intermediate temperature range is illustrated in Fig. 4 by temperature dependences of both $1/\chi$ and μ_{eff}. At about 33 K long range magnetic order sets-in.

More information about the magnetic ordering phenomena has been obtained from AC susceptibility studies. In these studies a small measuring AC field of the order of 1 Oe and a measuring field frequency of 430 Hz have been employed. The magnetic ordering takes places in stages as there are two pronounced ordering events, at $T_N = 33$ K and at $T_C = 27$ K. A remarkable feature of the latter transition is the extremely sharp and sizable imaginary susceptibility χ'' peak, a fingerprint of the onset of strongly dissipative magneto-dynamics, see Fig. 5.

4. Discussion on the magnetic properties

As one could expect from the complex crystal structure, involving four crystallographically different Co atoms, the magnetic properties of $Co_7(TeO_3)_4Br_6$ are complex as well. The complexity applies both to the broad temperature range above magnetic orderings and to the ordering itself. A detailed interpretation of the magnetic structure and mechanisms ruling the magnetic behaviour of $Co_7(TeO_3)_4Br_6$ is very demanding and will not be attempted in this study. Instead, we present here just the general framework that we find relevant for basic understanding of magnetic properties of the compound.

A most remarkable feature in the paramagnetic state is a pronounced deviation from CW behaviour. There are several

possible reasons for the later deviation, from the reduced effective magnetic dimensionality, disordering effects of impurities, to the possibility of temperature dependent repopulation of various spin states, to name a few. However, the most common cause for the deviation stems from magnetic features of single Co^{2+} ions in an octahedral ligand field. As it is well-known for certain 3d configurations (in particular for d^1, d^2, d^6 and d^7) the single ion susceptibility is, in principle, strongly temperature dependent [21,22]. In some cases the temperature dependence may reveal a CW-like form. The single ion contribution relies on the energy splitting ('zero-field splitting') between the t_{2g} and e_g 3d orbitals introducing, in turn, a g-factor anisotropy [20–22]. Assuming the presence of ligand field effects Curie–Weiss formalism becomes a misleading concept for the interpretation of the observed $\chi(T)$ dependence as it has nothing to do with cooperative magnetic phenomena. However, as magnetic order undoubtedly sets-in below 35 K, cooperative magnetic correlations are present in the system far above 35 K. While in the intermediate temperature range single ion effects prevent us from any insight into these correlations the high-temperature CW behaviour might be consistent, in view of θ_{CW} being negative in sign (Fig. 4), with antiferromagnetic spin correlations. Accordingly, the cusp-like anomaly at $T_N = 33$ K could be interpreted as an evidence of AF ordering transition. The second sharply peaked anomaly at $T_C = 27$ K can only be attributed, due to its size and sharpness, to three-dimensional ferromagnetic or, perhaps, ferrimagnetic ordering. It is therefore quite probable to expect presence of the coexisting antiferromagnetic and ferromagnetic correlations in the magnetic structure of $Co_7(TeO_3)_4Br_6$.

The most striking element in magnetic ordering represents however the 'explosion' of imaginary susceptibility χ'', just at the temperature at which long-range ferromagnetic (or ferrimagnetic) order has been established, see Fig. 5. To the best of our knowledge such an observation has not been reported so far for any compound before. Generally, non-zero χ'' tells about the presence of dissipative magnetic excitations in the system: induced sample magnetization then lags in phase behind the applied low-frequency field due to transfer of energy to the lattice. Generally, transfer of energy from magnetic system can be mediated by some relaxation or resonance mechanism, usually in the radio-frequency range [20]. As the frequency of our applied AC field is orders of magnitude lower we interpret the observed feature of χ'' in a traditional framework of the dissipative domain-wall motion. Indeed, dissipation sets-in just at the point of ferromagnetic domains formation. However, the size and sharpness of the effect requires additional studies in order to characterize the properties of the domain-wall pinning potential and other involved mechanisms responsible for such a unique feature of the $Co_7(TeO_3)_4Br_6$ magnetism.

At present we can only speculate about the magnetic structure of $Co_7(TeO_3)_4Br_6$ and the involved interactions at the microscopic level. It seems reasonable to assume that the magnetic structure might be determined by the layered crystal structure (and planar sample morphology) rendering the effective magnetism two-dimensional. This possibility will be a subject for future investigations.

5. Conclusions

Large single crystals of the new compound $Co_7(TeO_3)_4Br_6$ in form of platelets with a size of $10 \times 10 \times 0.1$ mm^{-3} were synthesized by a chemical transport reaction in sealed and evacuated silica tubes from CoO, TeO_2, $CoBr_2$ in the off-stoichiometric molar ratio 4 : 3 : 2 with HBr as transporting agent. The charge and growth-zone temperatures were 600 and 400 °C respectively. Also $Co_7(TeO_3)_4Cl_{3.6}Br_{2.4}$ single crystals were grown from the same starting mixture but with HCl as transporting agent over the temperature gradient 600 to 450 °C. The new compounds are isostructural and crystallise in the centrosymmetric monoclinic space group C2/c. The structure can be described as layered in the bc-plane. The layers are built by edge and corner sharing $[CoO_4Br_2]$ octahedra and via corner sharing to $[TeO_3E]$ tetrahedra. The layers are joined by $[CoO_2Br_4]$ octahedra. Non-bonding regions are formed were the lone pairs on Te^{4+} and the Br atoms are located.

The magnetic properties of $Co_7(TeO_3)_4Br_6$ are characterized by $3d^7$, $S = 3/2$, spin state and magnetic susceptibility strongly deviating from the Curie–Weiss behaviour in a broad temperature range. Below 35 K there are two successive magnetic transitions, attributed to antiferromagnetic and ferromagnetic (or ferrimagnetic) magnetic orderings, respectively. The latter magnetic ordering is accompanied by intriguing magnetic dynamics.

Supplementary material

Supplementary material for $Co_7(TeO_3)_4Br_6$ has been sent to Fachinformationzentrum Karlsruhe, Abt. PROKA, 76344 Eggenstein-Leopoldshafen, Germany (fax +49 7247 808 666; e-mail: crysdata@fiz-karlsruhe.de), and can be obtained on quoting the deposit number CSD-416145.

Acknowledgements

This work has in part been carried out with financial support from the Swedish Research Council. The work in Lausanne was supported by the Swiss National Science Foundation (SNSF) and by the MaNEP while the work in Zagreb was supported by the resources of the SNSF-SCOPES project. We are grateful to Prof. D. Pavuna for stimulating comments and discussions.

References

[1] M. Johnsson, K.W. Törnroos, F. Mila, P. Millet, Chem. Mater. 12 (2000) 2853.
[2] M. Johnsson, K.W. Törnroos, Acta Cryst. C 59 (2003) i53.
[3] M. Johnsson, K.W. Törnroos, Solid State Sci. 5 (2003) 263.
[4] M. Johnsson, K.W. Törnroos, P. Lemmens, P. Millet, Chem. Mater. 15 (2003) 68.
[5] R. Becker, M. Johnsson, R. Kremer, P. Lemmens, J. Solid State Chem. 178 (2005) 2024.
[6] P. Lemmens, K.Y. Choi, E.E. Kaul, C. Geibel, K. Becker, W. Brenig, R. Valenti, C. Gros, M. Johnsson, P. Millet, F. Mila, Phys. Rev. Lett. 87 (2001), 227201-1.
[7] M. Prester, A. Smontara, I. Zivkovic, A. Bilusic, D. Drobac, H. Berger, F. Bussy, Phys. Rev. B 69 (2004), 180401-1.

[8] P. Lemmens, G. Gűntherodt, C. Gros, Phys. Rep. 376 (2003) 1, and references therein.
[9] R. Becker, H. Berger, M. Johnsson, M. Prester, Z. Marohnic, M. Miljak, M. Herak, J. Solid State Chem. 179 (2006) 836.
[10] R. Becker, M. Johnsson, Solid State Sci. 6 (2004) 519.
[11] X-RED, version 1.22, STOE & Cie GmbH, Darmstadt, Germany, 2001.
[12] X-SHAPE, version 1.06, STOE & Cie GmbH, Darmstadt, Germany, 1999.
[13] G.-M. Sheldrick, SHELXS-97—program for the solution of crystal structures, Göttingen, 1997.
[14] G.-M. Sheldrick, SHELXL-97—program for the refinement of crystal structures, Göttingen, 1997.
[15] C.R. Feger, J.W. Kolis, Inorg. Chem. 37 (1998) 4046.
[16] R. Takagi, M. Johnsson, Acta Cryst. C 61 (2005) i106.
[17] T.F. Semenova, I.V. Rozhdestvenskaya, S.K. Filatov, L.P. Vergasova, Mineralog. Magazine 56 (1992) 241.
[18] S.V. Krivovichev, S.K. Filatov, T.F. Semenova, I.V. Rozhdestvenskaya, Zeitschrift fuer Kristallographie 213 (1998) 645.
[19] P.S. Berdonosov, D.G. Shabalin, A.V. Olenev, L.N. Demianets, V.A. Dolgikh, B.A. Popovkin, J. Solid State Chem. 174 (2003) 111.
[20] S. Blundell, Magnetism in Condensed Matter, Oxford Univ. Press, New York, 2001.
[21] S. Hatscher, H. Schilder, H. Lueken, W. Urland, Pure Appl. Chem. 77 (2005) 497.
[22] J.S. Griffith, The Theory of Transition Metal Ions, Cambridge Univ. Press, Cambridge, 1971.